Available online at www.sciencedirect.com
SCIENCE DIRECT
Polymer 46 (2005) 7519–7527
polymer
www.elsevier.com/locate/polymer

Molecular modeling and simulation of ion-conductivity in chitosan membranes

Ernesto López-Chávez*, José Manuel Martínez-Magadán, Raúl Oviedo-Roa, Javier Guzmán, Joel Ramírez-Salgado, Jesús Marín-Cruz

Programa de Ingeniería Molecular, Instituto Mexicano del Petróleo, Eje Central Lázaro Cárdenas 152, México D.F. 07730, México

Received 19 October 2004; received in revised form 25 April 2005; accepted 30 April 2005
Available online 1 July 2005

Abstract

The objective of this work is to provide some elements for developing a theoretical methodology aimed to describe the ion conductivity mechanism of chitosan membrane and to obtain its magnitude. Atomistic molecular modeling has been utilized to construct an ionic-conducting polymer–electrolyte system consisting of chitosan, H_2O molecules and H_3O^+, OH^-, SO_4^{2-} ions, inside of the simulation cell. The COMPASS force field was used. The simulation allows describing the ionic conductivity mechanism along the polymer matrix. The theoretical results obtained are compared with previously reported experimental data for chitosan membranes. The present methodology can be considered as a first step towards understanding these complex problems of technological interest.

Keywords: Ion-conductivity; Polyelectrolyte; Chitosan membrane

1. Introduction

Chitosan is a polyelectrolyte derived from chitin, the second biopolymer most abundant in the nature only after the cellulose, through a deacetylation process. Chitin is well known to consist of 2-acetamido-2-deoxy-β-D-glucose groups by a β (1–4) linkage. Thus, chitosan is the *N*-deacetylated derivate of chitin, although this *N*-deacetylation is almost never complete [1]. The chitosan macromolecule has unique properties [2] as a consequence of the presence of both amino and hydroxyl groups in their structure, as shown in Fig. 1.

The comprehension of both ionic conduction mechanism and ionic conductivities of the hydrated chitosan membranes are very important in developing alkaline polymer electrolyte or acidic polymer electrolyte fuel cells. Hither to, there has been a minimal amount of experimental work conducted to address ionic conductivity in chitosan polyelectrolyte membranes. To our knowledge, there is no theoretical effort dealing with this issue. Within the framework of experimental domain, Wan et al. [3] have reported measurements of the intrinsic ionic conductivity on chitosan membranes with various degrees of deacetylation and different molecular weights. The values that they have found were as high as 10^{-4} S cm^{-1} after hydration for 1 h. On the other hand, Soontarapa et al. [4] have prepared four types of chitosan membranes for investigating their electrochemical properties. The membranes were unscrosslinked, 1 and 2% crosslinked, and acid-doped membranes. The conductivity at 100% of relative humidity under H_2 atmosphere was measured within a temperature range of 40–80 °C. It was found that the conductivity of the 2% doped membrane with 1% H_2SO_4 was a half of that of Nafion® 117 at all temperatures. However, theoretical work for the chitosan membranes is null practically.

Polyelectrolyte membranes have been extensively investigated lately due to their potential applications in different types of electrochemical devices such as solid non-corrosive electrolytes [5]. As ion conducting membranes in fuel cells [6], electrolyte polymers have been used over the past three decades. For the case of application in fuel cells, a primary goal is to find polymer materials with ion conductivities within the range of mS/cm at temperatures up to 100 °C. Electrolytes containing different ions such as

* Corresponding author. Tel.: +52 55 5729 6139.
E-mail address: elopezc@esfm.ipn.mx (E. López-Chávez).

0032-3861/$ - see front matter © 2005 Elsevier Ltd. All rights reserved.
doi:10.1016/j.polymer.2005.04.107

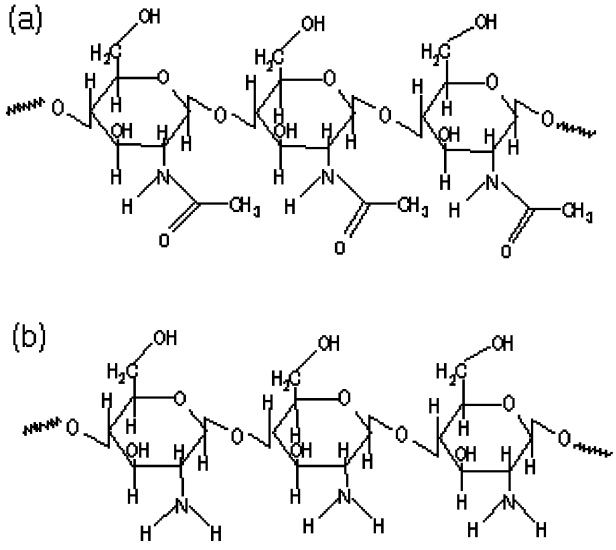

Fig. 1. Segments of (a) chitin and (b) chitosan.

sulfonic, hydronium, hydroxide, oxide and carbonate ions as charge carriers are known, and are the basis for the many categories of fuel cells under development today [7].

Ion conduction is a thermally activated process and its magnitude varies dramatically from one material to the other. The type of electrolyte, which may be either liquid or solid, determines the temperature at which the fuel cell may be operated. The main limitation to obtain a polymeric material with a high value of conductivity at high temperatures is necessary to maintain the polymeric membrane hydrated, since their ionic conductivity increases linearly with the water content, the membrane reaches the maximum conductivity when it is completely hydrated. Nevertheless, the obtained results to date are quite promising. Polymers classes for this type of applications such as poly(ethylene oxide), poly(vinylalcohol), poly-(acrylamide), poly(vinylpyrrolidone), poly(ethyleneimine), various poly(aminosilicates), and poly(benzimidazole) have been examined in combination with sulfuric, phosphoric and various halide acids [8].

Due to its capacity of water retention, the chitosan has recently emerged as a new alternative to obtain membranes with high ionic conductivity at moderate temperatures, >90 °C, for fuel cells operation. Chitosan membrane loses its water content around 110 °C [9]. Another important advantage of this polymer is that their behavior can be changed significantly by modifying the hydroxyl and amine groups or the residual acetamide groups by NH_3, CH_2OH, PO_3H, or SO_3H ones, with suitable chemical methods [10], so that ionic conductivity of the chitosan membrane can be improved. Chitosan also has a high potential for development into sophisticated functional polymers quite different from those of synthetic polymers since it has both free amino groups and hydroxyl groups on its backbone, which are easily modified by many organic reactions [11,12] As copolymer, chitosan is readily converted to fibers, films, coatings, and beads as well as powders and solutions further enhancing its usefulness [13].

The conduction mechanism in chitosan membranes is partly unknown at present and the experimental work has not, despite many efforts, been able to resolve all the atomistic-level details. To our best knowledge, there are few works devoted to theoretical prediction of the ionic conduction mechanism of polyelectrolyte, among them stand out the realized by Ennari et al. [14–16]. The rapid increase in computing resources and the progress in software offer new possibilities to rapidly gain new information from molecular modeling and simulation of the conductivity phenomena.

In the present study, molecular dynamics (MD) atomistic simulations of an ion-conducting system, consisting of two chain-polymeric (each one with 12 amino groups protonated-chitosan monomers), one hydronium ion, one hydroxide ion, 200 water molecules and 12 sulfate ions, was constructed to study the ionic conductivity of both hydronium and hydroxide ions. This system could be constructed of the following way: when a chitosan film is formed after the evaporation of acetic acid, the amino groups are protonated. Besides, a sodium sulfate solution produces the dissociation of both SO_4^{2-} and Na^+ ions. If the sulfates are added to protonated chitosan membrane and the sodium ions are removed, then the system used in this work is constituted.

The MD was realized by using COMPASS forcefield [17], which is the first ab initio forcefield that has been parameterized and validated using condensed-phase properties, in addition to various ab initio and empirical data for isolated molecules. Consequently, this forcefield enables accurate prediction of structural, conformational, vibrational, ionic conductivity and thermo physical properties for a broad range of molecules in isolation and in condensed phases.

The present work looks to find a general methodology that could be applied to any polymer electrolyte membrane, besides it could turn out to be a reliable, economical and useful tool to the design and synthesis process of this type of membranes which are used in many technological applications.

2. Methodology

The methodology used in this work was based on a procedure previously reported by Ennari et al. for studying proton-conducting polymer electrolyte system consisting of poly(ethylene oxide) sulfonic acid anion [11–13]. In this work, the amorphous builder module of Accelrys was used to construct polymeric membrane/small molecule penetrant system. The minimization and molecular dynamics simulations were carried out using discover molecular simulation program. In order to obtain both the ionic conduction mechanism and the ionic conductivities of the hydrated

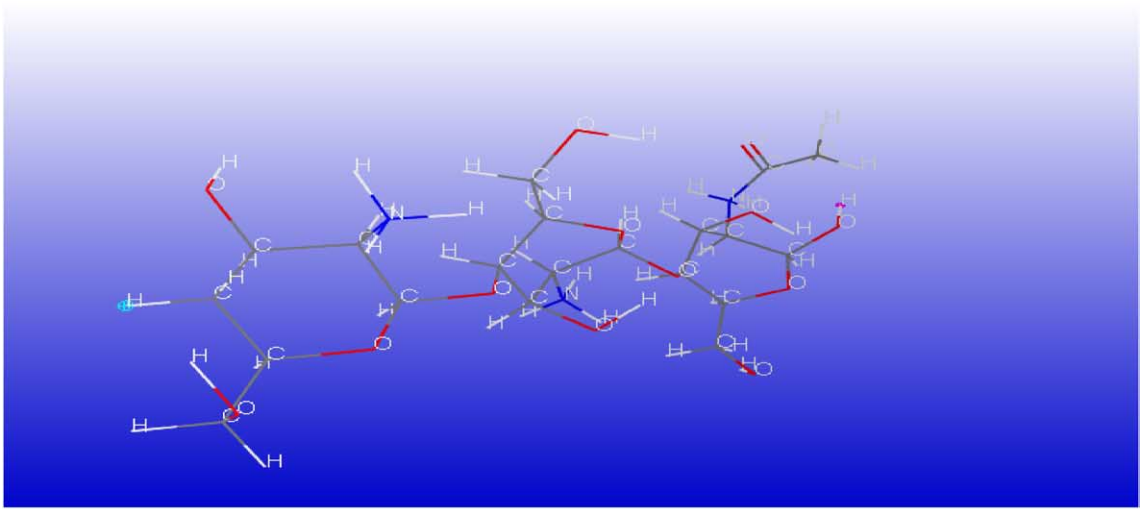

(a) Protonated Chitosan structure.

(b) Water molecule (H_2O)

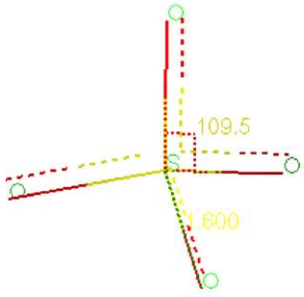

(c) Sulphate ion ($SO_4^=$)

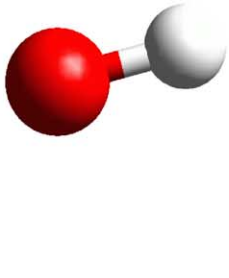

(d) Hydroxide ion (OH^-)

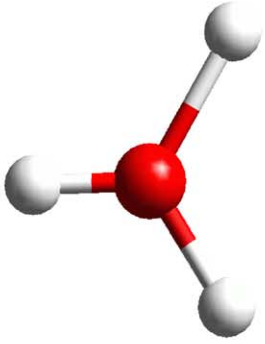

(e) Hydronium ion (H_30^+)

Fig. 2. Elements used in the simulation cell.

chitosan membranes, the following computational scheme is proposed: one starting structure within a 3D cell with periodic boundary conditions was built using the amorphous builder code from MSI (Accelrys, Inc.) [18]. The system studied consisted of two parallel polymeric-chains each one with 12 amino groups protonated chitosan monomers, which were constructed with the polymer code [19], one hydronium ion, one hydroxide ion, 200 water molecules and 12 sulfate ions, all these elements are shown in the Fig. 2, whereas the complete simulation cell is presented in the Fig. 3. The simulation cell final density was 0.1520 g/cm^3 and the dielectric constant is 78. The simulation cell size was $50\times50\times60$ Å^3 corresponding to an average volume of $\langle V\rangle = 1.5\times10^5$ Å^3. The number of atoms inside the system is 1834, where there are 984 H, 288 C, 48 N, 490 O and 24 S atoms. All calculations were made using the COMPASS forcefield.

The cell was first minimized with molecular mechanics using the steepest-descents method. After minimization, a molecular dynamics run was made using the NVT ensemble and the Nose [20] method for temperature control. The temperature used in the dynamics was 298 °K. The time step was 0.01 ps. The charge equilibration procedure (Q_{eq}) of Rappe and Goddard [21] was applied to determine all partial atomic charges. Ewald summation was used to calculate the long-range interactions in all bulk phase MD simulations. All non-bond interactions were directly treated using cutoff distance of 25 Å.

The electric conductivity, σ, due to the transport of hydronium and hydroxide ions, has been evaluated by using the Einstein equation [22]:

$$\sigma = \frac{e^2}{6tVkT}\left(\sum_i z_i^2\langle\|\mathbf{R}_i(t)-\mathbf{R}_i(0)\|^2\rangle + 2\sum_{k>l} z_k z_l\langle\|\mathbf{R}_k(t)-\mathbf{R}_k(0)\|\,\|\mathbf{R}_l(t)-\mathbf{R}_l(0)\|\rangle\right) \quad (1)$$

where e is the elemental charge, t is observation time, V is the volume of the cell, k is the Boltzmann constant, T is the temperature, z_i is the total charge in units of e for the diffusing ion whose mass-center position vector is $\mathbf{R}_i$. The first term of the right-hand side is the charge-weighted sum over each ion mean square displacement, and the later term is the sum of correlation of displacements of ions describing the interactions between different ions. Fig. 4 depicts the classic equivalent of the molecular system, i.e. the ions are considered as point charges and the interactions among them are of ion–ion, ion–dipole and dipole–dipole types.

The COMPASS/MD simulation generates a set of positions for all atoms in the cell for instants $t=n$ft, being n an integer and ft the discrete step for the dynamics simulation. We have chosen a value of ft = 0.01 ps and n ranging from 1 to 13,048. The time average in Eq. (1) for any $f(t)$ function (e.g. $\|\mathbf{R}_i(t)-\mathbf{R}_i(0)\|^2$) is simply defined as $\langle f(t)\rangle = \frac{1}{n}\sum_{i=1}^{n} f(i)$. The symbol $\|\mathbf{r}\|$ denotes the magnitude of vector $\mathbf{r}$.

3. Results and discussion

Molecular dynamics simulations were started from rest for the resulting optimized structure of the system within the forcefield approximation.

Fig. 5 shows a sequence of snapshots which describe clearly the ionic conduction mechanism through the membrane as a result of the process of mobility of the charge-carrier ionic species. The snapshot simulation times are: 0, 1, 2.46, 22.15 and 41.85 ps. During the simulation process, it was observed that the hydronium and hydroxide ions suffered three types of movement: rotational, translational and vibration, even though the conductivity was different, both high and low. Fig. 5(a) shows the positions of all the atoms, molecules and ions of the system, at the moment in which the process of molecular dynamics was initiated. In this figure it is possible to appreciate that molecules of water and the charge-carrier ionic species (hydronium, hydroxide and sulfate) are concentrated in the region in which the charge density of the polymeric chains pair of chitosan is smaller. Because the NH_3^+ groups are bonded to the backbone, only hydronium, hydroxide and sulfate ions are free to move and give a contribution to the ionic conductivity of the system.

Figs. 6 and 7 show a sequence of frames in which the translation, rotation, vibration of hydroxide and hydronium ions, respectively, can be observed. The green arrow represents the velocity vector in the current time and the number of its magnitude in Å/ps. These types of movement

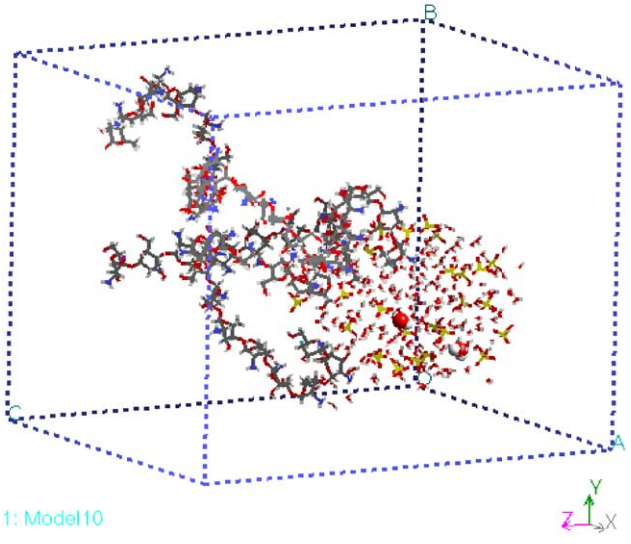

Fig. 3. A snapshot from the molecular dynamic simulation of cell.

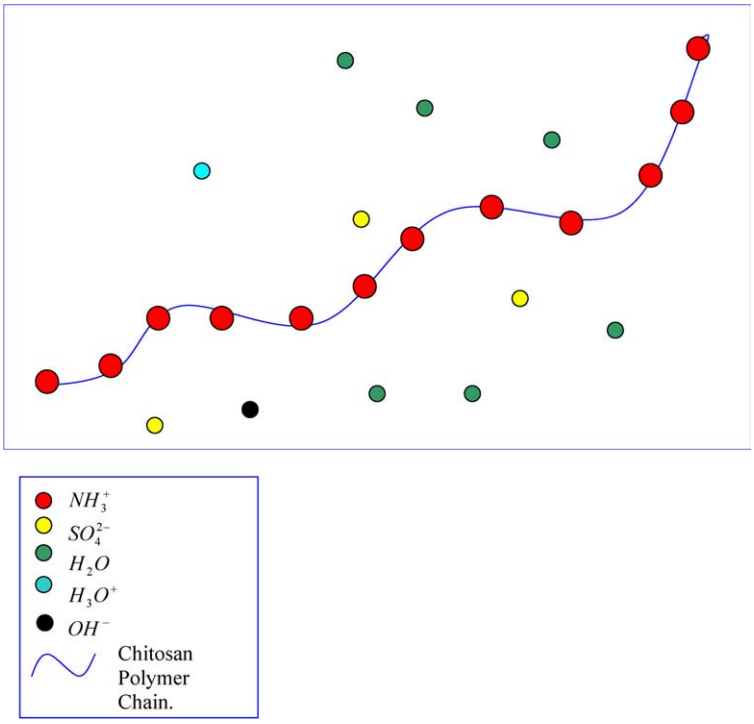

Fig. 4. Schematic representation of the studied system. The ions are considered as point charge and the interactions among them are of type ion–ion, ion–dipole and dipole–dipole.

depend on the above mentioned ion–ion, ion–dipole and dipole–dipole interactions, and they determine the total ionic conductivity of the membrane.

In Fig. 8, time evolution of both total and average conductivity is shown, moreover, hydronium and hydroxide ions separation distance is also presented. The separation distance between hydronium and hydroxide was obtained considering the file of the positions of hydronium and hydroxide ions. This file was generated from molecular dynamic simulations. Once the positions file was generated, a program in Fortran language was built for calculating the distance by means of the formula: $\|\mathbf{R}_{H_3O}(t) - \mathbf{R}_{OH}(t)\|^2$. This plot indicates that the different interactions, which have been carried out by system particles, instigate that such ions are further apart each time thus modifying the global conductivity.

On other hand, it is observed during early simulation moments, a relatively small total system conductivity (~ 0.4 S m^{-1}). The two first snapshots of Fig. 5, at $t=0$, and $t=1$ ps, are in correspondence with this result. In these pictures it can be observed that both hydroxide and hydronium ions initiate with low mobility. The hydroxide is preferably surrounded only by water molecules, whereas hydronium is surrounded by sulfate ions as well as water molecules. Here, hydroxide–water interactions are attractive and ion–dipole type. In addition, ion–ion repulsive interactions between hydroxide–sulfate are stronger than those hydroxide–hydronium attractive ones. The protonated amino groups of the chitosan do not still have, at this point, a considerable effect neither on hydroxide, nor on hydronium mobility. In the hydronium case, the attractive hydronium–sulfate interactions predominate over both hydronium–hidroxide repulsive interaction and water–hydronium ion–dipole interactions. Also, hydronium–hydroxide attractive interactions are relatively small, in these initial conditions, in accordance with its separation distances (Fig. 8).

In the Fig. 5(a), which corresponds to simulation time instant of 1 ps and to the first peak of the curve of conductivity of Fig. 8, it is appraised that due to the thermal variations, both hydronium and hydroxide begin to free themselves of the ‘fastenings’ that make them almost immovable, then charge carriers begin to move slowly. In addition, they begin to separate a little and move in opposite directions, giving origin to a small increase in the conductivity until reaching the first local maximum that appears in Fig. 8.

Nevertheless, Fig. 5(c), which corresponds to the time of simulation of 2.46 ps and to the first minimum of the curve of conductivity of Fig. 8, it is observed that later, hydronium and hydroxide are maintained almost static, they are oscillating slowly around an equilibrium position. Besides, it is observed that these two conductive ionic species approach slightly because its attractive interaction surpasses instantly to its interactions with other particles. Simultaneously, those others sulfates are directed towards some of the protonated amine groups of the polymeric chains, this

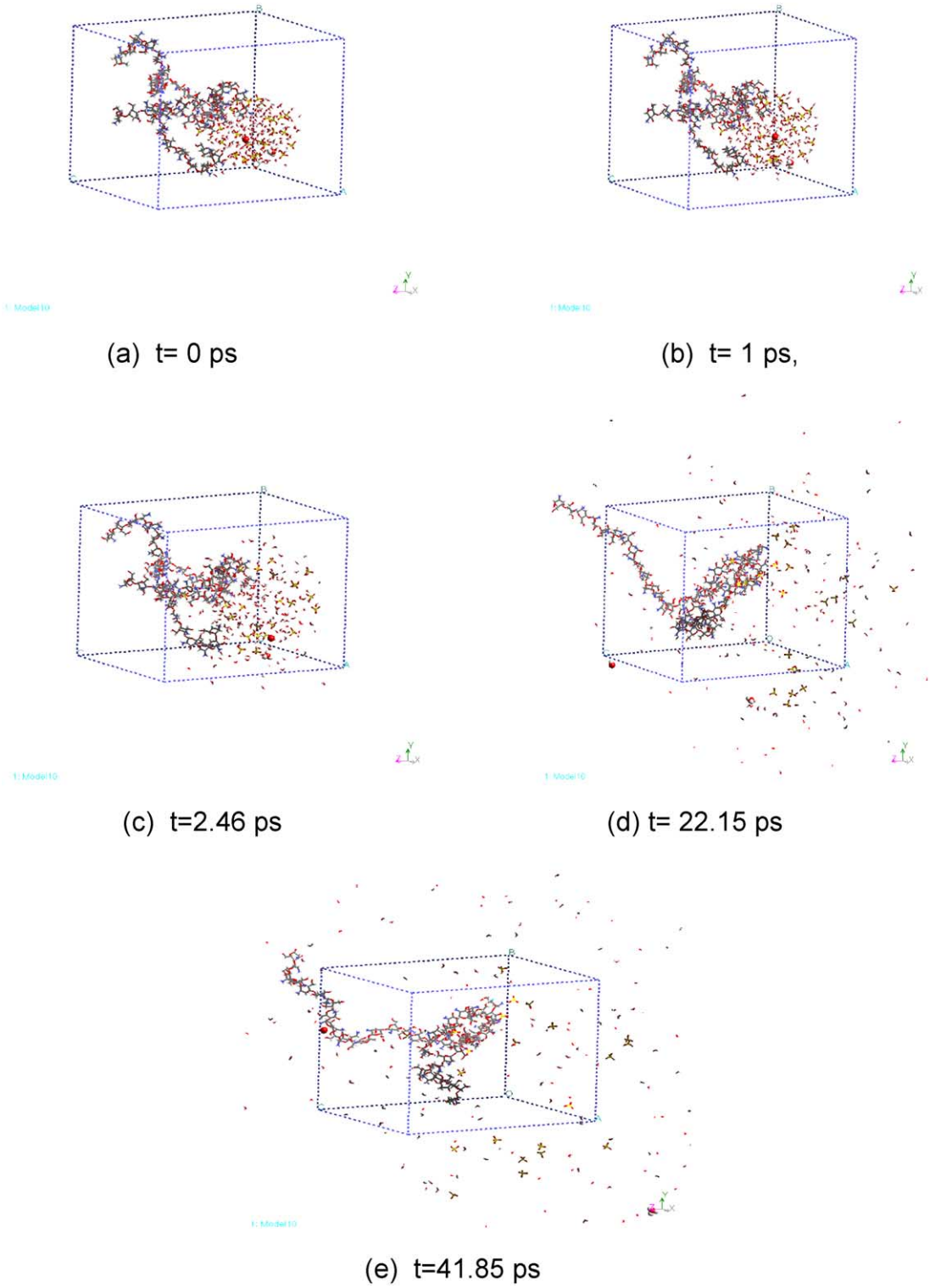

Fig. 5. Sequence of images that describes the ionic conduction mechanism of the membrane as well as the process of mobility of the charge carrier ionic species. The images correspond to times of simulation: 0, 1, 2.46, 22.15 and 41.85 ps.

situation causes a small decrement in the total conductivity of the system during the time interval of 1–2.46 ps, which is also appreciated in Fig. 8.

Once thermal equilibrium is reached around 22.15 ps, both hydronium and hydroxide are freed of their mutual attractive interaction, they begin to acquire greater mobility, moving in opposed trajectories. It can be observed in Fig. 5(d), in these conditions. Furthermore, we observe mainly that the sulfates, which have been anchored in some of the amino groups, lead the mobility of both hydroxide

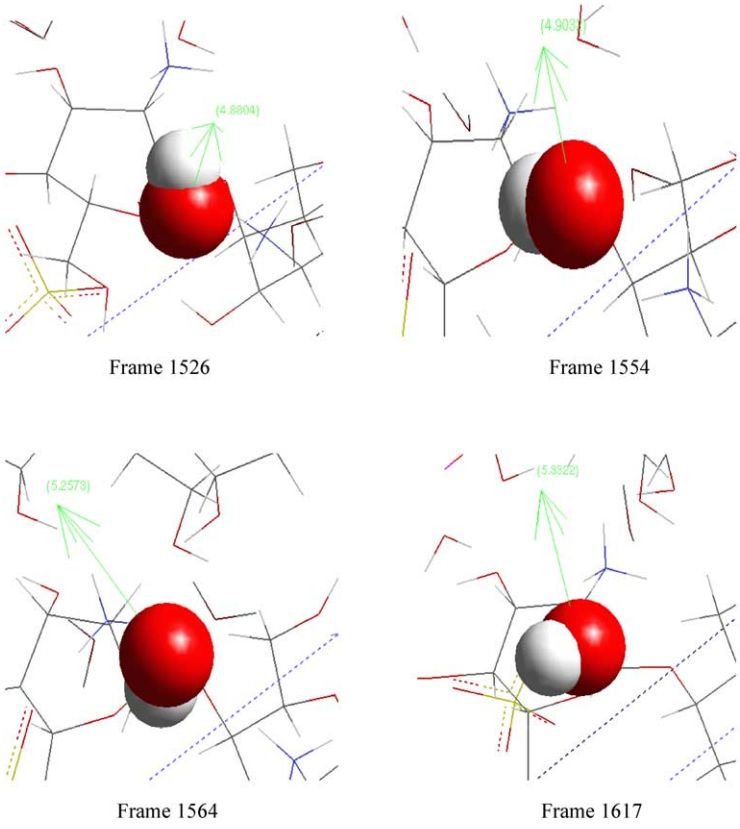

Fig. 6. Variation of hydroxide ion velocity in function of time. The green arrow represents the velocity vector in the current time and the number of its magnitude in Å/ps.

and hydronium through coulombian interactions of the type ion–ion. This situation considerably favors the conductivity of the system, which is observed in the conductivity graph. According to the conductivity graph and Fig. 6(d), which represent the situation at time 22.15 ps where the next prominent peak occurs, it is observed that the ionic species hydroxide and hydronium have a high mobility. During the time interval 2.46–22.15 ps, where they almost move in opposite directions causing an increase in the total conductivity of the system from 2.46 to 22.15 ps. Here it is possible to emphasize that the sulfates anchored in the amino groups of the membrane are those that continue leading the mobility of the charge carrier ionic species (Fig. 9). This situation agrees with one reported experimentally by Wan et al. [23] who found that the mechanism for ionic conductivity through the membranes may come from the function of free amine groups in the chitosan backbone.

Finally, the next minimum of Fig. 8 corresponding to the situation at time $t=41.85$ ps, which is shown in the Fig. 5(e). In this image, we found that for very long times of simulation, the mobility of the ionic species tends to become stabilized, being able to find the average value of the conductivity for all the system. The average value of the conductivity calculated from the data of simulation and using Eq. (1) is 2×10^{-2} S cm^{-1} with an error of about 2.0×10^{-4} S cm^{-1}.

When we compared our results against those obtained experimentally, it was found that in the works carried out by Wan et al. [3,22,24,25] the chitosan membranes had a ionic conductivity value from 10^{-5} to 10^{-3} S cm^{-1}. The membranes evaluated include different specimens such as membranes with different degree of deacetylation and molecular weights [3]; some hydroxyalquil derivatives [22], crosslinked chitosan membrane with epichlorohydrin and glutaraldehyde as reticulating agents [24]; phosphorylated chitosan membranes [25]. All membranes were evaluated in dry and wet states by electrochemical impedance spectroscopy, obviously the best ionic conductors were the wet membranes.

On the other hand, Herranen et al. [26] experimentally obtained the conductivity of poly(ethylene oxide) PEO sulfonic acid anion and PEO containing membrane. The obtained values using impedance measurements were 1.5×10^{-3} S cm^{-1} at relative humidity (RH) 75.3% and 1.5×10^{-5} S cm^{-1} at RH 38.2%. Ennari et al. [27] carried out a simulation of this system in order to find the factors that improve its conductivity. They predict that the increase of water in

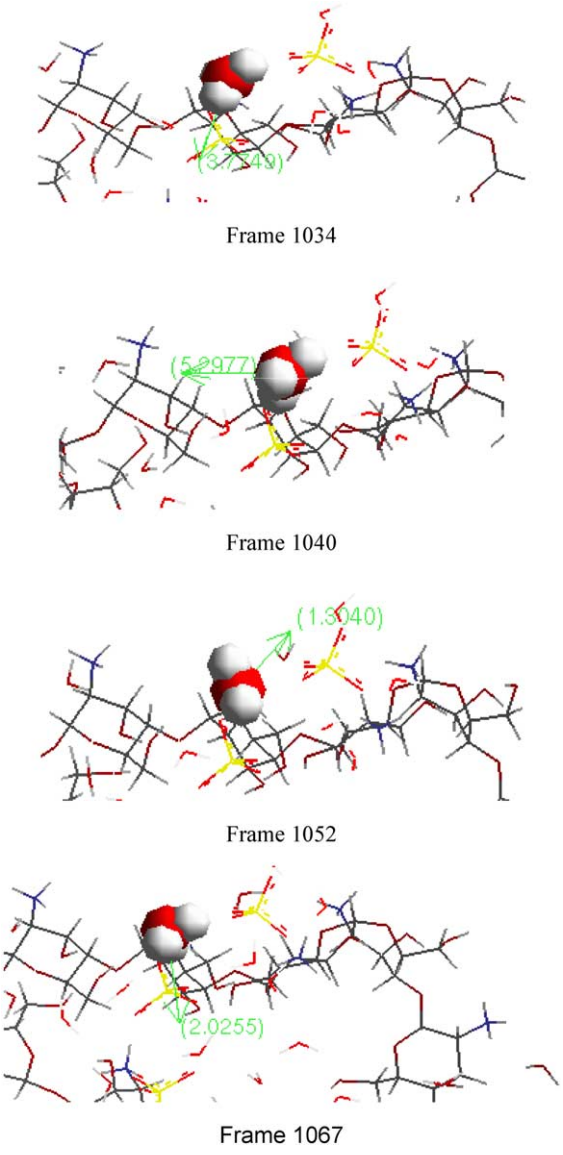

Fig. 7. Variation of hydronium velocity in function of time. The green arrow represents the velocity vector in the current time and the number its magnitude in Å/ps.

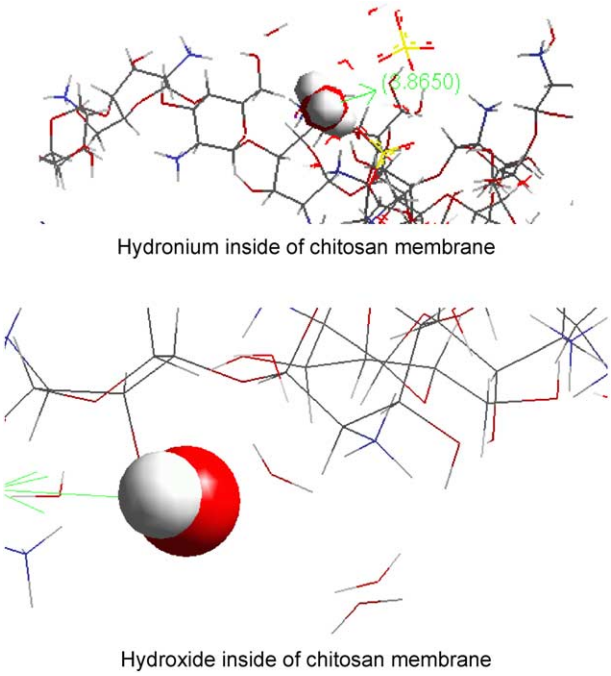

Fig. 9. Behavior of hydronium and hydroxide ions inside the chitosan membrane.

the system might favor that the conductivity values increase of the PEO until 2.6×10^{-2} S cm^{-1}, which is of the same order of magnitude than we obtained in this work.

Finally Smitha et al. [28] demonstrated that the polyelectrolyte membranes made of chitosan protonated (cationic) and poly-acrilic acid (anionic) could reach a proton conductivity as high as 3.8×10^{-2} S cm^{-1}. They found the ideal composition for the membrane is 50% of chitosan and 50% of poly-acrilic acid, this membrane has low methanol permeation and good mechanical properties.

The values of ionic conductivity reported in the two last works (Ennari et al. [27] and Smitha et al. [28]) are in the same order of magnitude than we obtained in this work.

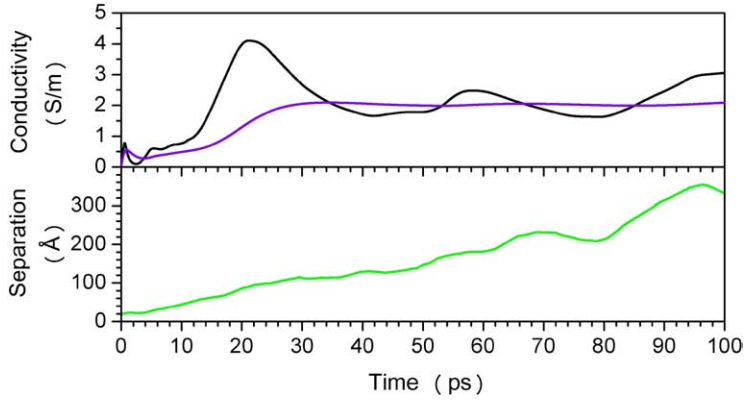

Fig. 8. Total conductivity and average conductivity as a function of time, the black line represents the total conductivity whereas the violet line is the average conductivity. The curve green corresponds to the distance of separation between hydronium and hydroxide as a function of time.

4. Conclusions

We have presented general ideas to develop a theoretical methodology, based on molecular simulations and considering a great number of atoms for studying the ionic conductivity mechanism of polymer-based conducting materials.

A simulation cell consisting of two parallel polymeric-chains each one with 12 protonated chitosan monomers, one hydronium ion, one hydroxide ion, 200 water molecules and 12 sulfate ions was constructed in order to study the ion-conductivity of chitosan membranes. The results were compared with that obtained by the experimental work for similar materials and by molecular modeling for previously studied another polyelectrolyte systems and show good agreement with the results reported in the present work.

To study the mechanism of the ionic conductivity in the system, three ionic species were used: hydronium, hydroxide and sulfate ions. The hydronium and the hydroxide are ionic species that present movement along the polymer matrix. We observe that the sulfates anchored in the amino groups of the membrane backbone lead the mobility of the charge carrier ionic species. This is in agreement with one reported experimentally.

These studies suggest that the percent of water and sulfates may improve the ionic conductivity in chitosan membranes until a value of $2\times10^{-2}\,\mathrm{S\,cm^{-1}}$. This work goes directly to find a general methodology that could be applied to any polymer-based conducting material, further it could turn out to be reliable, economical and it could result in a useful tool for evaluating new materials by experimentalists.

Acknowledgements

This study is supported by IMP Project D.00142. The authors would like to thank Paige Guzman for your review of language.

References

[1] Ravi Kumar MNV. React Funct Polym 2000;46:1.
[2] Hudson SM. Advances in chitin science. In: Domard A, Roberts GAF, Varum K, editors. Proceedings of the 7th international conference on chitin and chitosan, vol. 2. Lyon, France: Jaques Andre; 1997. p. 590.
[3] Wan Y, Creber KAM, Peppley B, Tam Bui V. Polymer 2003;44:1057.
[4] Soontarapa K, Suwan N, Ota KI, Mitsushima S, Kamiya N. 'Development of polyeletrolyte based proton exchange membrane' 9th APPChE Congress and CHEMECA 29 September–3 October, paper #345. Christchurch, New Zealand: Christchurch Convention Centre; 2002 [http://www.cape.canterbury.ac.nz/webdb/Apcche_Proceedings/APCChE/Data/345REV.pdf].
[5] Chen-Yang YW, Hwang JJ, Chang FH. Macromolecules 1997;30:3825.
[6] Bohn HG, Schober T. J Am Ceram Soc 2000;83:768.
[7] Larmine J, Andrews D. Fuel cell systems explained. Chichester: Wiley; 2000.
[8] Haile SM. Acta Mater 2003;51:5981.
[9] Kordesch K, Simader G. Fuel cells and their applications. Weinheim, Germany: VCH; 1996.
[10] Kurita K. Prog Polym Sci 2001;26:1921.
[11] Terbojevich M, Carrazo C, Aosani A. Makromol Chem 1989;190:2847.
[12] Kallio T, Lundstrom M, Sundholm G, Walsby N, Sundholm F. Appl Electrochem 2002;32:11.
[13] Phillip B, Dautzenberg H, Linow KJ, Kotz J. Prog Polym Sci 1989;14:91.
[14] Ennari J, Elomaa M, Sundholm F. Polymer 1999;40:5035.
[15] Ennari J, Neelov I, Sundholm F. Comput Theor Polym Sci 2000;10:403.
[16] Ennari J, Elomaa M, Neelov I, Sundholm F. Polymer 2000;41:985.
[17] Sun H, Ren P, Fried JR. Comput Theor Polym Sci 1998;8:229.
[18] Brown D, Clarke JHR. Macromolecules 1991;24:2075.
[19] Polymer user guide, version 4.00, San Diego, Molecular Simulation Inc (1998). April 1998. San Diego, CA: MSI; 1998.
[20] Nose S. J Chem Phys 1984;81:511.
[21] Rappe AK, Goddard WA. J Phys Chem 1985;95:3358.
[22] Muller-Plathé F. Acta Polym 1994;45:259.
[23] Wan Y, Creber KAM, Peppley B, Bui BT. J Polym Sci, Part B: Polym Phys 2004;42:1379.
[24] Wan Y, Creber KAM, Peppley B, Bui BT. J Appl Polym Sci 2003;89:306.
[25] Wan Y, Creber KAM, Peppley B, Bui BT. Macromol Chem Phys 2003;204:850.
[26] Herranen J, Kinnunen J, Mattsson B, Rinne H, Sundholm F, Torrel L. Solid State Ion 1995;80:201.
[27] Ennari J, Neelov I, Sundholm F. Polymer 2001;42:8043.
[28] Smitha B, Sridhar S, Khan AA. Macromolecules 2004;37:2233.